Bull. Aust. Math. Soc. **112** (2025), 290–302
doi:10.1017/S000497272400128X

THE DENSE REGION IN SCATTERING DIAGRAMS

TIM GRÄFNITZ and PATRICK LUO

(Received 11 October 2024; accepted 16 November 2024; first published online 10 February 2025)

Abstract

We use deformations and mutations of scattering diagrams to show that a scattering diagram with initial functions $f_1 = (1 + tx)^\mu$ and $f_2 = (1 + ty)^\nu$ has a dense region. This answers a question asked by Gross and Pandharipande ['Quivers, curves, and the tropical vertex', *Port. Math.* **67**(2) (2010), 211–259] which had been proved only for the case $\mu = \nu$.

2020 *Mathematics subject classification*: primary 14J33; secondary 13F60.

Keywords and phrases: scattering diagram, mirror symmetry, cluster algebra, quiver representation.

1. Introduction

Scattering diagrams (introduced in [13]) are a method to combinatorially encode families of automorphisms of an algebraic torus (or, more generally, elements of the Lie group associated to a pronilpotent Lie algebra). They are related to various subjects such as curve counting [1, 2, 4, 6, 10, 14], quiver representations [9, 16], stability conditions [3, 5], cluster algebras [8, 14] and mirror symmetry [7, 11–13].

A *scattering diagram* $\mathfrak{D}$ (in dimension two) is a collection of rays $\mathfrak{d} \subset \mathbb{R}^2$ with attached functions $f_\mathfrak{d} \in \mathbb{C}[x^{\pm 1}, y^{\pm 1}][\![t]\!]$. It is completely described by the coefficients $c_{a,b}$ of its functions. We use the factorised representation

$$f_\mathfrak{d} = \prod_{k>0} (1 + tx^a y^b)^{c_{ka,kb}}.$$

Each ray or line $\mathfrak{d}$ induces an automorphism $\theta_\mathfrak{d} \in \mathrm{Aut}_{\mathbb{C}[\![t]\!]}\mathbb{C}[x^{\pm 1}, y^{\pm 1}][\![t]\!]$. Starting with an initial diagram $\mathfrak{D}_0$, there is a scattering algorithm that iteratively produces scattering diagrams $\mathfrak{D}_k$ such that the composition of the automorphisms $\theta_\mathfrak{d}$ is trivial modulo t^k. Taking the formal limit, one obtains a *consistent* scattering diagram $\mathfrak{D}_\infty$. (See Section 2.1 for more details.)

The aim of this paper is to show that most consistent scattering diagrams have a *dense region* in which, for every slope, there exists a ray with nontrivial function

This project was financially supported by Mark Gross' ERC Advanced Grant Mirror Symmetry in Algebraic Geometry (MSAG).

© The Author(s), 2025. Published by Cambridge University Press on behalf of Australian Mathematical Publishing Association Inc.

https://doi.org/10.1017/S000497272400128X Published online by Cambridge University Press

$f_{\mathfrak{d}} \neq 1$. To achieve this, we make use of three different techniques using certain properties of scattering diagrams.

First (Section 2.2 and [8, 10]), we can assume that no more than two rays or lines intersect in the same point. Otherwise, one can *deform* the diagram by slightly moving its rays. If a ray $\mathfrak{d}$ has a reducible function $f_{\mathfrak{d}} = f_1 \cdots f_r$, one can also split it into several rays with irreducible functions $f_1, \ldots, f_r$ and then deform the diagram to obtain nonintersecting parallel rays $\mathfrak{d}_1, \ldots, \mathfrak{d}_r$.

Second (Section 2.3 and [8]), using a *change of lattice* we can assume that the two rays or lines intersect transversally, so that the attached functions are $f_1 = (1 + tx)^{\mu}$ and $f_2 = (1 + ty)^{\nu}$. The corresponding consistent diagram is called a *standard scattering diagram* $\mathfrak{D}^{\mu,\nu}$. By the above, it suffices to study standard scattering diagrams.

Third (Section 2.4 and [8, 9]), the rays in a standard scattering diagram $\mathfrak{D}^{\mu,\nu}$ obey certain symmetries related to the notion of *mutations*. Precisely, the corresponding coefficients satisfy $c^{\mu,\nu}_{a,b} = c^{\mu,\nu}_{\mu b-a,b} = c^{\mu,\nu}_{a,\nu a-b}$.

We use the above techniques to prove the theorem stated below.

DEFINITION 1.1. Let $\mathfrak{D}^{\mu,\nu}$ be a standard scattering diagram, that is, the consistent diagram obtained from the initial diagram consisting of two lines with functions $f_1 = (1 + tx)^{\mu}$ and $f_2 = (1 + ty)^{\nu}$. The function attached to the ray in $\mathfrak{D}^{\mu,\nu}$ with direction (a, b), $\gcd(a, b) = 1$, can be factorised as

$$f^{\mu,\nu}_{(a,b)} = \prod_{k>0} (1 + tx^a y^b)^{c^{\mu,\nu}_{ka,kb}},$$

defining positive integers (by Proposition 2.9) $c^{\mu,\nu}_{ka,kb} \in \mathbb{Z}_{>0}$.

DEFINITION 1.2. Define (μ,ν)-mutations $\mathbf{T}^{\mu,\nu}_1(a, b) = (\mu b - a, b), \mathbf{T}^{\mu,\nu}_2(a, b) = (a, \nu a - b)$.

DEFINITION 1.3. We say that $(a, b) \in \mathbb{Z}^2_{>0}$ is in the dense region $\Phi^{\mu,\nu}$ if

$$\frac{\mu\nu - \sqrt{\mu\nu(\mu\nu - 4)}}{2\mu} < \frac{b}{a} < \frac{\mu\nu + \sqrt{\mu\nu(\mu\nu - 4)}}{2\mu}.$$

THEOREM 1.4.

(a) *If $(a, b) \in \mathbb{Z}^2_{>0}$ is in the dense region $\Phi^{\mu,\nu}$, then $c^{\mu,\nu}_{a,b} \neq 0$.*

(b) *Otherwise, $c^{\mu,\nu}_{a,b} \neq 0$ if and only if (a, b) is obtained from $(1, 0)$ or $(0, 1)$ via a sequence of (μ, ν)-mutations. In particular, (a, b) must be primitive in this case.*

Theorem 1.4 will be proved in Section 3. The idea is as follows. It is enough to show density inside a fundamental domain $\phi^{\mu,\nu}_0$ for the mutation actions (Section 3.1). One can show that $\phi^{\mu+1,\nu}_0$ (respectively, $\phi^{\mu,\nu+1}_0$) is contained in $\Phi^{\mu,\nu}$ if $\mu\nu > 4$ and $\mu > 1$ (respectively, $\nu > 1$). Then, by induction and symmetry $\mu \leftrightarrow \nu$, it is enough to show density for $\Phi^{2,3}$ and $\Phi^{1,5}$ (Section 3.2). We show this explicitly by deforming $\mathfrak{D}^{2,3}$ to $\mathfrak{D}^{2,2}$ plus $\mathfrak{D}^{2,1}$ and deforming $\mathfrak{D}^{1,5}$ to $\mathfrak{D}^{1,3}$ plus $\mathfrak{D}^{1,2}$ (Section 3.3). Part (b) follows from the mutation actions (Section 3.4).

https://doi.org/10.1017/S000497272400128X Published online by Cambridge University Press

REMARK 1.5. Theorem 1.4 answers [9, Question 4]. It was proved in the case $\mu = \nu$ in [9, Section 4.7], using an existence statement for quiver representations from [15]. Reineke stated that there should be a similar argument in the case $\mu \neq \nu$ using bipartite quivers [18], but this has not been worked out in detail. Our proof is purely combinatorial.

2. Preliminaries

2.1. Scattering diagrams. We provide a definition for scattering diagrams, based on [10]. (See [8, 10] for more general definitions.)

Let $M \cong \mathbb{Z}^2$ be a lattice with basis $e_1 = (1, 0), e_2 = (0, 1)$, and let $N := \mathrm{Hom}_{\mathbb{Z}}(M, \mathbb{Z})$. For $m \in M$, let $z^m \in \mathbb{C}[M]$ denote the corresponding element in the group ring. If $x = z^{e_1}, y = z^{e_2}$, then $\mathbb{C}[M] = \mathbb{C}[x^{\pm 1}, y^{\pm 1}]$ is the ring of Laurent polynomials in x and y.

Let R be an Artin local $\mathbb{C}$-algebra with maximal ideal $\mathfrak{m}_R$, and let

$$\mathbb{C}[M]\widehat{\otimes}_{\mathbb{C}}R = \varprojlim \mathbb{C}[M] \otimes_{\mathbb{C}} R/\mathfrak{m}_R^k.$$

We take $M = N = \mathbb{Z}^2$ and $R = \mathbb{C}[\![t]\!]$, so that $\mathbb{C}[M]\widehat{\otimes}_{\mathbb{C}}R = \mathbb{C}[x^{\pm 1}, y^{\pm 1}][\![t]\!]$ and $\mathfrak{m}_R = (t)$.

DEFINITION 2.1. A *ray* or *line* is a pair $\mathfrak{d} = (\underline{\mathfrak{d}}, f_{\mathfrak{d}})$, where $\underline{\mathfrak{d}} = b_{\mathfrak{d}} + \mathbb{R}_{\geq 0} m_{\mathfrak{d}}$ if it is a ray or $\underline{\mathfrak{d}} = b_{\mathfrak{d}} + \mathbb{R} m_{\mathfrak{d}}$ if it is a line, and $f_{\mathfrak{d}} \in \mathbb{C}[z^{m_{\mathfrak{d}}}]\widehat{\otimes}_{\mathbb{C}}R \subseteq \mathbb{C}[M]\widehat{\otimes}_{\mathbb{C}}R$ is a function such that

$$f_{\mathfrak{d}} \equiv 1 \pmod{z^{m_{\mathfrak{d}}}\mathfrak{m}_R}.$$

A *scattering diagram* $\mathfrak{D}$ is a collection of rays and lines such that, for every $k > 0$, there are finitely many rays and lines $(\underline{\mathfrak{d}}, f_{\mathfrak{d}})$ with $f_{\mathfrak{d}} \not\equiv 1 \pmod{\mathfrak{m}_R^k}$.

DEFINITION 2.2. For a ray $\mathfrak{d}$ and a curve γ in $M_{\mathbb{R}}$ intersecting $\mathfrak{d}$ transversally at p, let $n_{\mathfrak{d}} \in N$ annihilate $m_{\mathfrak{d}}$ and evaluate positively on $\gamma'(p)$. Define $\theta_{\mathfrak{d}} = \theta_{\gamma,p,\mathfrak{d}} \in \mathrm{Aut}_{\mathbb{C}[\![t]\!]}(\mathbb{C}[M]\widehat{\otimes}_{\mathbb{C}}R)$ by

$$\theta_{\mathfrak{d}} : z^m \mapsto z^m f_{\mathfrak{d}}^{\langle m, n_{\mathfrak{d}} \rangle}.$$

DEFINITION 2.3. A *singularity* of a scattering diagram $\mathfrak{D}$ is either a base point of a ray or an intersection between two rays or lines that consists of a single point.

Let $\gamma : [0, 1] \to M_{\mathbb{R}}$ be a smooth curve that does not pass through any singularities and whose endpoints are not in any ray or line in the diagram. If all intersections of γ with rays or lines are transverse, then we define the *γ-ordered product* $\theta_{\gamma,\mathfrak{D}} \in \mathrm{Aut}_R(\mathbb{C}[M]\widehat{\otimes}_{\mathbb{C}}R)$ in the following way. For each k, as there are finitely many rays or lines with functions $f_{\mathfrak{d}} \not\equiv 1 \pmod{\mathfrak{m}_R^k}$, let $0 < p_1 \leq p_2 \leq \cdots \leq p_s < 1$ be such that, at each p_i, $\gamma(p_i) \in \mathfrak{d}_i$ for some ray or line $(\mathfrak{d}_i, f_{\mathfrak{d}_i})$, and when $p_i = p_j$ for $i \neq j$, $\mathfrak{d}_i \neq \mathfrak{d}_j$ are different rays of the diagram. Then let $\theta_i = \theta_{\gamma,p_i,\mathfrak{d}_i}$ and

$$\theta_{\gamma,\mathfrak{D}}^k = \theta_s \circ \cdots \circ \theta_2 \circ \theta_1.$$

Then we define $\theta_{\gamma,\mathfrak{D}}$ as the formal limit $\theta_{\gamma,\mathfrak{D}} = \lim_{k\to\infty}(\theta_{\gamma,\mathfrak{D}}^k)$.

https://doi.org/10.1017/S000497272400128X Published online by Cambridge University Press

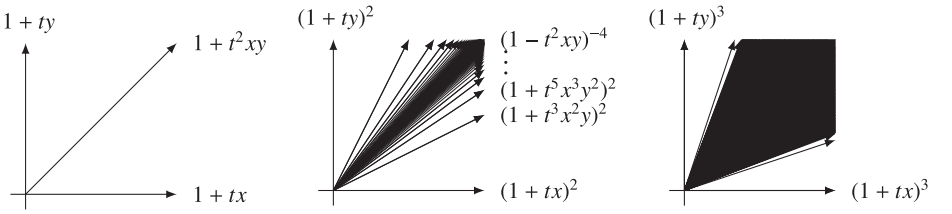


FIGURE 1. The standard scattering diagrams $\mathfrak{D}^{1,1}$, $\mathfrak{D}^{2,2}$ and $\mathfrak{D}^{3,3}$.

We say that a diagram $\mathfrak{D}$ is *consistent* if $\theta_{\gamma,\mathfrak{D}}$ is the identity map for every closed curve γ (for which $\theta_{\gamma,\mathfrak{D}}$ is defined). Two diagrams $\mathfrak{D}$ and $\mathfrak{D}'$ are *equivalent* if $\theta_{\gamma,\mathfrak{D}} = \theta_{\gamma,\mathfrak{D}'}$ for every curve γ.

PROPOSITION 2.4 [13], [10, Theorem 1.4]. *For a scattering diagram $\mathfrak{D}$, there exists a consistent scattering diagram $\mathfrak{D}_\infty \supseteq \mathfrak{D}$ such that $\mathfrak{D}_\infty \setminus \mathfrak{D}$ consists only of rays.*

REMARK 2.5. The consistent diagram $\mathfrak{D}_\infty$ obtained from $\mathfrak{D}$ is unique (up to equivalence) if we require that it has no two rays $\mathfrak{d}, \mathfrak{d}'$ with the same support $\underline{\mathfrak{d}} = \underline{\mathfrak{d}}'$.

DEFINITION 2.6. If a consistent diagram $\mathfrak{D} = \mathfrak{D}_\infty$ has only one singularity, then (by Remark 2.5, up to equivalence) there is at most one ray in each direction $m \in \mathbb{Z}^2$. We write the function of this ray as $f_m^{\mathfrak{D}}$. If $f_m^{\mathfrak{D}} = 1$, then we can omit the ray.

DEFINITION 2.7. The *standard scattering diagram* $\mathfrak{D}^{\mu,\nu} = \mathfrak{D}_\infty^{\mu,\nu}$ is the diagram obtained by performing scattering on the initial diagram

$$\mathfrak{D}_0^{\mu,\nu} = \{(\mathbb{R}(1,0), (1+tx)^\mu), (\mathbb{R}(0,1), (1+ty)^\nu)\}.$$

The scattering only produces rays in the first quadrant, that is, with $m_{\mathfrak{d}} = (a,b) \in \mathbb{Z}^2_{>0}$. Consider an equivalent diagram to a standard scattering diagram such that there is a unique ray in each direction (see Remark 2.5). We can express the function $f_{\mathfrak{d}}$ of the ray $\mathfrak{d}$ in direction $(a,b) \in \mathbb{Z}^2_{>0}$ as

$$f^{\mu,\nu}_{(a,b)} := f^{\mathfrak{D}^{\mu,\nu}}_{(a,b)} = \prod_{k=1}^{\infty} (1 + t^{ka+kb} x^{ka} y^{kb})^{c^{\mu,\nu}_{ka,kb}}.$$

DEFINITION 2.8. The *coefficients* for $\mathfrak{D}^{\mu,\nu}$ are these $c^{\mu,\nu}_{a,b}$.

PROPOSITION 2.9 [8, Proposition C.13]. *The coefficients of a standard scattering diagram are positive integers: $c^{\mu,\nu}_{a,b} \in \mathbb{Z}_{>0}$.*

REMARK 2.10. Note that $c^{\mu,\nu}_{a,b} = c^{\nu,\mu}_{b,a}$ by symmetry: as $\mathfrak{D}^{\mu,\nu}_\infty$ is consistent, its reflection along the diagonal $\mathbb{R}(1,1)$ is as well, which gives a consistent diagram containing $\mathfrak{D}^{\nu,\mu}_0$.

EXAMPLE 2.11. Figure 1 shows the standard scattering diagrams $\mathfrak{D}^{1,1}$, $\mathfrak{D}^{2,2}$ and $\mathfrak{D}^{3,3}$.

The diagram $\mathfrak{D}^{1,1}$ has, apart from the initial lines, only one ray in direction $(1,1)$ with function $f^{1,1}_{(1,1)} = 1 + t^2xy$. Hence, the only nontrivial coefficient is $c^{1,1}_{1,1} = 1$.

https://doi.org/10.1017/S000497272400128X Published online by Cambridge University Press

The diagram $\mathfrak{D}^{2,2}$ has only rays in directions $(1,1)$, $(n,n+1)$ and $(n+1,n)$ for $n \in \mathbb{N}$, with

$$f^{2,2}_{(1,1)} = (1-xy)^{-4}, \quad f_{(n,n+1)} = (1+x^n y^{n+1})^2, \quad f_{(n+1,n)} = (1+x^{n+1}y^n)^2.$$

Hence, the nonzero coefficients $c^{2,2}_{a,b}$ are

$$c^{2,2}_{n,n} = \begin{cases} 4 & n = 2^k, \\ 0 & \text{otherwise}, \end{cases} \qquad c^{2,2}_{n,n+1} = 2, \quad c^{2,2}_{n+1,n} = 2.$$

In particular, the rays are discrete.

For $\mathfrak{D}^{3,3}$ there is a *dense region* in which each ray appears with nontrivial function. This is the statement of Theorem 1.4. The functions $f^{3,3}_{(a,b)}$ and coefficients $c^{3,3}_{a,b}$ are very complicated and unknown in general. Only for the slope 1 coefficients $c^{\mu,\nu}_{k,k}$ is there a known formula, which was proved for $\mu = \nu$ in [17, Theorem 6.4] and for $\mu \neq \nu$ in [18, Corollary 11.2]. (See also [10, Example 1.6] and [9, Section 1.4].)

2.2. Deformations. Given a consistent scattering diagram $\mathfrak{D}$, we can form the asymptotic diagram $\mathfrak{D}_{\text{as}}$ by replacing every ray $(b_{\mathfrak{d}} + \mathbb{R}_{\geq 0} m_{\mathfrak{d}}, f_{\mathfrak{d}})$ with $(\mathbb{R}_{\geq 0} m_{\mathfrak{d}}, f_{\mathfrak{d}})$, and similarly for lines. By considering sufficiently large curves in $\mathfrak{D}$ around the origin containing all singularities, we see that $\mathfrak{D}_{\text{as}}$ is also consistent. We can use this to consider *deformations* as follows. (For more details see [10, Section 1.4] and [8, Proposition C.13, Step III].)

DEFINITION 2.12. The *full deformation* of $\mathfrak{D}^{\mu,\nu}$ consists of general lines $\mathfrak{d}_{1,1}, \dots, \mathfrak{d}_{1,\mu}$, $\mathfrak{d}_{2,1}, \dots, \mathfrak{d}_{2,\nu}$ with functions

$$f_{\mathfrak{d}_{1,i}} = 1 + tx, \quad f_{\mathfrak{d}_{2,i}} = 1 + ty.$$

Here the lines being general means that all rays in the consistent diagram intersect in points, not in rays. We will also consider *partial deformations* by pulling out only one factor.

PROPOSITION 2.13 [10, Section 1.4]. *Let $\mathfrak{D}'$ be a partial or full deformation of $\mathfrak{D}$. Then $(\mathfrak{D}'_\infty)_{\text{as}} = \mathfrak{D}_\infty$.*

EXAMPLE 2.14. Figure 2 shows a full deformation of $\mathfrak{D}^{3,1}$ and a partial deformation by pulling out one factor of $(1+x)^3$. This gives $c^{3,1}_{1,1} = 3$, $c^{3,1}_{2,1} = 3$, $c^{3,1}_{3,1} = 1$, $c^{3,1}_{3,2} = 3$.

LEMMA 2.15. *If $\mu \leq \mu'$ and $\nu \leq \nu'$, then $c^{\mu,\nu}_{a,b} \leq c^{\mu',\nu'}_{a,b}$.*

PROOF. Deform $\mathfrak{D}^{\mu',\nu'}$ in such a way that we have a horizontal line with function $(1+tx)^\mu$ and a vertical line with function $(1+ty)^\nu$. From this, we get a ray contributing $c^{\mu,\nu}_{a,b}$. As all coefficients are positive by Proposition 2.9, we see that $c^{\mu,\nu}_{a,b} \leq c^{\mu',\nu'}_{a,b}$. □

2.3. The change of lattice trick. There is a useful way to reduce to only needing to consider standard diagrams (found in [8, Proof of Proposition C.13, Step IV]).

https://doi.org/10.1017/S000497272400128X Published online by Cambridge University Press

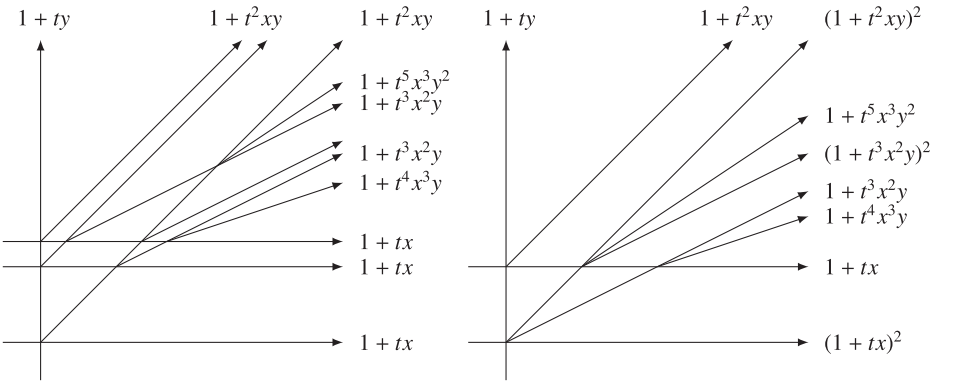


FIGURE 2. A full (left) and partial (right) deformation of $\mathfrak{D}^{3,1}$.

PROPOSITION 2.16. *Let $\mathfrak{D}$ be the consistent diagram obtained from the scattering diagram consisting of two lines $\mathfrak{d}_1$ and $\mathfrak{d}_2$ with functions $f_1 = (1 + tz^{m_1})^{d_1}$ and $f_2 = (1 + tz^{m_2})^{d_2}$. Let $M' \subseteq M$ be the sublattice generated by m_1 and m_2 and let $N' \supseteq N$ be the dual lattice. If $m \in M \setminus M'$, then $f_m = 1$. Otherwise, write $m = am_1 + bm_2$. Then*

$$f_m^{\mathfrak{D}} = (f_{(a,b)}^{d_1 e(m_2^*), d_2 e(m_1^*)})^{1/e(n)},$$

where $n \in N'$ is orthogonal to $m \in M'$ and primitive and, for any $n' \in N'$,

$$e(n') := \min\{k \in \mathbb{N} \mid kn' \in N\}.$$

In particular, the scattering of any scattering diagram consisting of two lines can be computed from a standard scattering diagram.

PROOF. Any ray $\mathfrak{d}$ in $\mathfrak{D}$ has direction vector $m_{\mathfrak{d}}$ contained in $M' \subseteq M$. Hence, we can consider $\mathfrak{d}$, $\mathfrak{D}$ and $\mathfrak{D}_\infty$ in the lattice M or in the lattice M'. In the latter case, we write $\mathfrak{d}'$, $\mathfrak{D}'$ and $\mathfrak{D}'_\infty$. By definition, the automorphism $\theta_{\mathfrak{d}} \in \mathrm{Aut}_{\mathbb{C}[\![t]\!]}(\mathbb{C}[M]\widehat{\otimes}_{\mathbb{C}}\mathbb{C}[\![t]\!])$ defined by a ray $\mathfrak{d} \in \mathfrak{D}_\infty$ is given by

$$\theta_{\mathfrak{d}} : z^m \mapsto z^m f_{\mathfrak{d}}^{\langle m, n_{\mathfrak{d}} \rangle}.$$

Let $e(n')$ be defined as above. Then we have $n_{\mathfrak{d}} = e(n_{\mathfrak{d}'})n_{\mathfrak{d}'}$ and the corresponding automorphism $\theta_{\mathfrak{d}'} \in \mathrm{Aut}_{\mathbb{C}[\![t]\!]}(\mathbb{C}[M']\widehat{\otimes}_{\mathbb{C}}\mathbb{C}[\![t]\!])$ defined by $\mathfrak{d}' \in \mathfrak{D}'_\infty$ is given by

$$\theta_{\mathfrak{d}'} : z^{m'} \mapsto z^{m'} f_{\mathfrak{d}}^{\langle m', n_{\mathfrak{d}} \rangle} = z^{m'} f_{\mathfrak{d}}^{e(n_{\mathfrak{d}'})\langle m', n_{\mathfrak{d}'} \rangle} = z^{m'} f_{\mathfrak{d}'}^{\langle m', n_{\mathfrak{d}'} \rangle}.$$

This shows that $f_{\mathfrak{d}'} = f_{\mathfrak{d}}^{e(n_{\mathfrak{d}'})}$. In particular, the initial functions f_1 and f_2 considered in the lattice M' are $f_1' = (1 + tx)^{d_1 e(m_2^*)}$ and $f_2' = (1 + ty)^{d_2 e(m_1^*)}$, where $x = z^{m_1}$ and $y = z^{m_2}$. These are the initial functions of the standard scattering diagram $\mathfrak{D}^{d_1 e(m_2^*), d_2 e(m_1^*)}$.

We know that scattering gives a consistent diagram $\mathfrak{D}_\infty^{d_1 e(m_2^*), d_2 e(m_1^*)}$. We get a consistent diagram containing $\mathfrak{D}$ by replacing any ray $\mathfrak{d}' \in \mathfrak{D}_\infty^{e(n_1), e(n_2)}$ by $\mathfrak{d}$ with function $f_{\mathfrak{d}} = f_{\mathfrak{d}'}^{1/e(n_{\mathfrak{d}'})}$. By uniqueness of consistent diagrams up to equivalence (Remark 2.5), this completes the proof. □

https://doi.org/10.1017/S000497272400128X Published online by Cambridge University Press

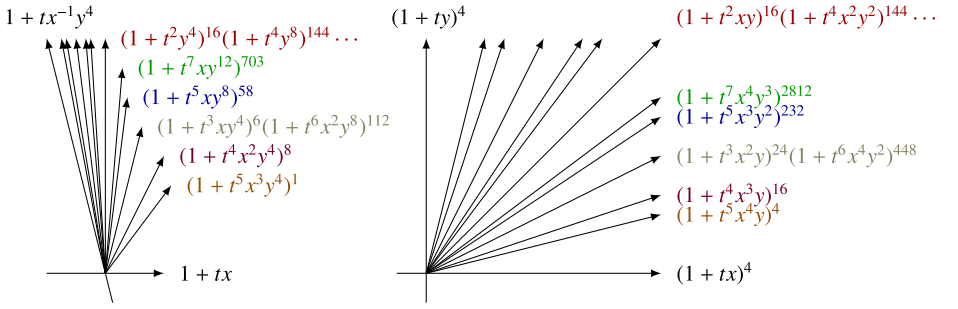


FIGURE 3. The diagrams $\mathfrak{D}^4_{\mathrm{det}}$ and $\mathfrak{D}^{4,4}$ to order seven.

EXAMPLE 2.17. Let $\mathfrak{D}^k_{\mathrm{det}}$ be the scattering diagram consisting of two lines with attached functions $f_1 = 1 + tx$ and $f_2 = 1 + tx^{-1}y^k$. Let M' be the sublattice generated by $m_1 = (1, 0)$ and $m_2 = (-1, k)$ and consider $m = am_1 + bm_2 \in M'$ primitive with dual $n \in N'$. Then

$$f_m^{\mathfrak{D}^k_{\mathrm{det}}} = (f_{(a,b)}^{k,k})^{\gcd(k,m_{(1)})/k},$$

where $m_{(1)}$ is the first component of $m \in M$. This is because we have $e(m_1^*) = e(m_2^*) = k$ and $e(n) = \gcd(k, m_{(1)})/k$. Figure 3 shows $\mathfrak{D}^k_{\mathrm{det}}$ and $\mathfrak{D}^{k,k}$ for $k = 4$ to t-order seven.

2.4. Mutations

DEFINITION 2.18. For $\mu, \nu \in \mathbb{Z}_{>0}$ define two *mutation* actions on $\mathbb{Z}^2$ by

$$\mathbf{T}_1^{\mu,\nu} : (a, b) \mapsto \begin{cases} (\mu b - a, b) & b > 0, \\ (a, b) & b \le 0, \end{cases} \quad \mathbf{T}_2^{\mu,\nu} : (a, b) \mapsto \begin{cases} (a, \nu a - b) & a > 0, \\ (a, b) & a \le 0. \end{cases}$$

Here $\mathbb{Z}^2$ is the space of direction vectors (a, b) of rays in a scattering diagram, and (a, b) will usually be assumed to be primitive, that is, $\gcd(a, b) = 1$, and such that (a, b), $\mathbf{T}_1^{\mu,\nu}(a, b)$ and $\mathbf{T}_2^{\mu,\nu}(a, b)$ are all contained in the first quadrant $\mathbb{Z}^2_{\ge 0}$.

PROPOSITION 2.19 [9, Theorem 7] and [8, Theorem 1.24]. *We have*

$$f^{\mu,\nu}_{(a,b)} = f^{\mu,\nu}_{\mathbf{T}_1^{\mu,\nu}(a,b)} = f^{\mu,\nu}_{\mathbf{T}_2^{\mu,\nu}(a,b)}.$$

3. Proof of Theorem 1.4

Consider a standard scattering diagram $\mathfrak{D}^{\mu,\nu}$ (Definition 2.7). Mutations (Section 2.4) act on the directions $\mathbb{Z}^2$ (or slopes $\mathbb{Q}$). They have some fixed points and naturally divide the scattering diagram into certain *regions*. We will show the following. All rays produced from scattering have slope $1/\mu < \rho < \nu$ (Proposition 3.13). For $\mu\nu > 4$, there is a *dense region* $\Phi^{\mu,\nu}$ between slopes $\rho_-^{\mu,\nu}$ and $\rho_+^{\mu,\nu}$ (Definition 3.1) in which

https://doi.org/10.1017/S000497272400128X Published online by Cambridge University Press

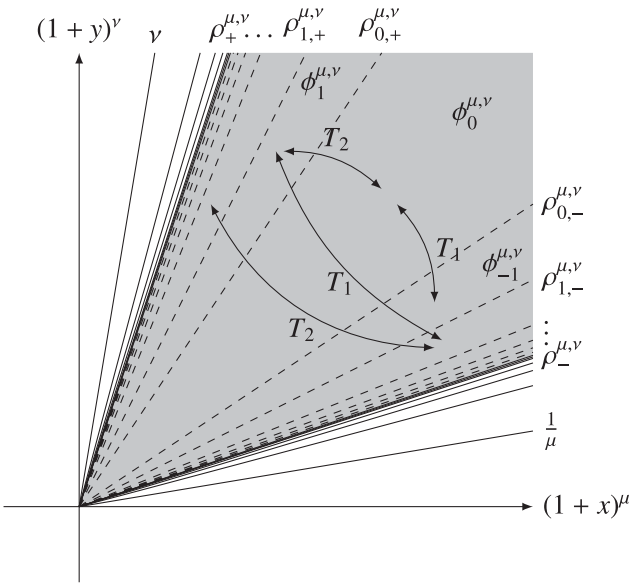


FIGURE 4. The regions of the scattering diagram.

every ray occurs with a nontrivial function (Theorem 3.3). It is made up of an infinite number of fundamental domains $\phi_k^{\mu,\nu}$ for the mutation action. The central domain $\phi_0^{\mu,\nu}$ lies between the slopes $\rho_{0,\pm}^{\mu,\nu}$ (Lemma 3.5). Outside the dense region there is a discrete number of rays and each of them appears with coefficients μ or ν, because they come from mutation of the initial rays (Proposition 3.14). The situation is summarised in Figure 4.

DEFINITION 3.1. In a standard scattering diagram $\mathfrak{D}^{\mu,\nu}$ where $\mu\nu > 4$, the *dense region* $\Phi^{\mu,\nu}$ is the cone spanned by the rays from the origin with slope

$$\rho_\pm^{\mu,\nu} = \frac{\mu\nu \pm \sqrt{\mu\nu(\mu\nu-4)}}{2\mu} = \frac{2\nu}{\mu\nu \mp \sqrt{\mu\nu(\mu\nu-4)}}.$$

A ray in direction $(a,b) \in \mathbb{Z}^2_{>0}$ is in the dense region if $\rho_-^{\mu,\nu} < b/a < \rho_+^{\mu,\nu}$.

In this section, we will prove the theorem stated below, by induction.

DEFINITION 3.2. A cone $\phi^{\mu,\nu} \subset \mathbb{R}^2_{>0}$ is *full* if $c_{a,b}^{\mu,\nu} \neq 0$ for every $(a,b) \in \mathbb{Z}^2_{>0}$ (not necessarily primitive) such that the ray in direction (a,b) lies in $\phi^{\mu,\nu}$.

THEOREM 3.3 (Theorem 1.4(a)). *$\Phi^{\mu,\nu}$ is full (and, in particular, dense with rays) when $\mu\nu > 4$.*

https://doi.org/10.1017/S000497272400128X Published online by Cambridge University Press

3.1. Fundamental domains

DEFINITION 3.4. The *fundamental region* $\phi_0^{\mu,\nu}$ is the cone between the directions

$$\rho_{0,+}^{\mu,\nu} = \frac{\nu}{2}, \quad \rho_{0,-}^{\mu,\nu} = \frac{2}{\mu}.$$

A ray in direction $(a, b) \in \mathbb{Z}_{>0}^2$ is in $\phi_0^{\mu,\nu}$ if $2/\mu \leq b/a \leq \nu/2$. For $k > 0$ and $k < 0$, define recursively

$$\rho_{k+1,+}^{\mu,\nu} = \mathbf{T}_1^{\mu,\nu}(\rho_{k,-}^{\mu,\nu}), \quad \rho_{k-1,-}^{\mu,\nu} = \mathbf{T}_2^{\mu,\nu}(\rho_{k,+}^{\mu,\nu}).$$

LEMMA 3.5. *The actions of* $\mathbf{T}_1^{\mu,\nu}$ *and* $\mathbf{T}_2^{\mu,\nu}$ *on the slope* $\rho = b/a$ *are order reversing (or strictly decreasing) for* $1/\mu < \rho < \nu$ *and have fixed points* $\rho_{0,-}^{\mu,\nu} = 2/\mu$ *and* $\rho_{0,+}^{\mu,\nu} = \nu/2$*, respectively.*

PROOF. This is clear from the definition (see Definition 2.18). The actions on the slope are given by

$$\mathbf{T}_1(\rho) = \frac{1}{\mu - 1/\rho}, \quad \mathbf{T}_2(\rho) = \nu - \rho. \qquad \square$$

LEMMA 3.6. *We have* $\mathbf{T}_1^{\mu,\nu}(\rho_+^{\mu,\nu}) = \rho_-^{\mu,\nu}$ *and* $\mathbf{T}_2^{\mu,\nu}(\rho_-^{\mu,\nu}) = \rho_+^{\mu,\nu}$.

PROOF. The second statement is

$$\mathbf{T}_2^{\mu,\nu}(\rho_-^{\mu,\nu}) = \nu - \frac{\mu\nu - \sqrt{\mu\nu(\mu\nu-4)}}{2\mu} = \frac{\mu\nu + \sqrt{\mu\nu(\mu\nu-4)}}{2\mu} = \rho_+^{\mu,\nu}.$$

For the first statement, we show that the reciprocals are equal,

$$\frac{1}{\mathbf{T}_1^{\mu,\nu}(\rho_+^{\mu,\nu})} = \mu - \frac{\mu\nu - \sqrt{\mu\nu(\mu\nu-4)}}{2\nu} = \frac{\mu\nu + \sqrt{\mu\nu(\mu\nu-4)}}{2\nu} = \frac{1}{\rho_-^{\mu,\nu}}. \qquad \square$$

LEMMA 3.7. *We have* $\lim_{k\to\infty} \rho_{k,\pm}^{\mu,\nu} = \rho_\pm^{\mu,\nu}$.

PROOF. The compositions $\mathbf{T}_1^{\mu,\nu}\mathbf{T}_2^{\mu,\nu}$ and $\mathbf{T}_2^{\mu,\nu}\mathbf{T}_1^{\mu,\nu}$ are strictly increasing continuous functions for $1/\mu < \rho < \nu$. Hence, they have unique fixed points, which, by Lemma 3.6, are given by $\rho_+^{\mu,\nu}$ and $\rho_-^{\mu,\nu}$. The limit of the recursively defined sequences $\rho_{k,-}^{\mu,\nu}$ and $\rho_{k,+}^{\mu,\nu}$ have to be fixed points of $\mathbf{T}_1^{\mu,\nu}\mathbf{T}_2^{\mu,\nu}$ and $\mathbf{T}_2^{\mu,\nu}\mathbf{T}_1^{\mu,\nu}$, respectively. Hence, they are given by $\rho_-^{\mu,\nu}$ and $\rho_+^{\mu,\nu}$. $\square$

LEMMA 3.8. *If* $\phi_0^{\mu,\nu}$ *is full, then so is* $\Phi^{\mu,\nu}$.

PROOF. By Lemmas 3.5, 3.6 and 3.7, $\Phi^{\mu,\nu}$ is the union of images of $\phi_0^{\mu,\nu}$ under repeated application of $\mathbf{T}_1^{\mu,\nu}$ and $\mathbf{T}_2^{\mu,\nu}$. This proves the claim. $\square$

3.2. Induction step

LEMMA 3.9. *If* $\mu\nu > 4$ *and* $\mu > 1$*, then* $\phi_0^{\mu+1,\nu}$ *is contained in* $\Phi^{\mu,\nu}$. *Similarly, if* $\mu\nu > 4$ *and* $\nu > 1$*, then* $\phi_0^{\mu,\nu+1}$ *is contained in* $\Phi^{\mu,\nu}$.

https://doi.org/10.1017/S000497272400128X Published online by Cambridge University Press

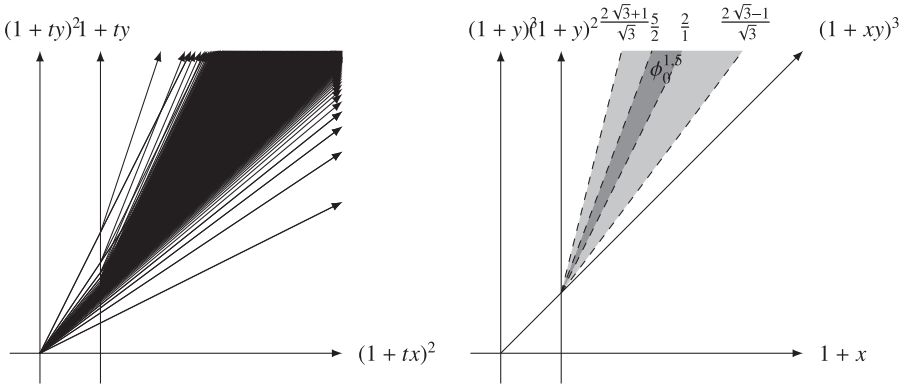


FIGURE 5. Partial deformations showing that $\phi_0^{2,3}$ (left) and $\phi_0^{1,5}$ (right) are full.

PROOF. By symmetry, we only have to show the second statement, which is equivalent to $\rho_{0,+}^{\mu,\nu+1} < \rho_+^{\mu,\nu}$ and $1/\rho_{0,-}^{\mu,\nu+1} < 1/\rho_-^{\mu,\nu}$. The second inequality is

$$\frac{\mu}{2} < \frac{\mu + \sqrt{\mu^2 - 4\frac{\mu}{\nu}}}{2} \iff 0 < \mu^2 - 4\frac{\mu}{\nu} \iff \mu\nu > 4.$$

The first inequality is

$$\frac{\nu+1}{2} < \frac{\nu + \sqrt{\nu^2 - 4\frac{\nu}{\mu}}}{2} \iff 1 < \nu^2 - 4\frac{\nu}{\mu} \iff \mu > \frac{4\nu}{\nu^2 - 1}.$$

For $\nu \geq 5$, the right-hand side is smaller than one, and hence any $\mu \in \mathbb{Z}_{>0}$ satisfies the inequality. For $\nu = 4, 3, 2$, the inequality is satisfied by all $\mu \geq 2, 2, 3$, respectively. Hence, all $\mu, \nu \in \mathbb{Z}_{>0}$ satisfying $\mu\nu > 4$ and $\nu > 1$ also satisfy this inequality. This completes the proof. □

PROPOSITION 3.10. *If $\Phi^{2,3}$ and $\Phi^{1,5}$ are full, then $\Phi^{\mu,\nu}$ is full for all $\mu\nu > 4$.*

PROOF. Start with a pair (μ, ν) with $\mu\nu > 4$. With $\mu\nu > 4$ do the following. If $\mu \geq \nu$, replace (μ, ν) by $(\mu - 1, \nu)$. Otherwise, replace (μ, ν) by $(\mu, \nu - 1)$. Doing this repeatedly we eventually arrive at $(1, 5)$ or $(5, 1)$ or $(2, 3)$ or $(3, 2)$. Note that, if $\mu\nu > 4$ and $\mu \geq \nu$, then $\mu > 1$. Similarly, if $\mu\nu > 4$ and $\nu > \mu$, then $\nu > 1$. By Lemmas 3.8 and 3.9, we conclude that $\Phi^{\mu,\nu}$ is full if $\Phi^{1,5}$, $\Phi^{5,1}$, $\Phi^{2,3}$ and $\Phi^{3,2}$ are full. By Remark 2.10, $\Phi^{5,1}$ is full if and only if $\Phi^{1,5}$ is full and $\Phi^{3,2}$ is full if and only if $\Phi^{2,3}$ is full. Hence, the statement follows. □

3.3. The base cases

LEMMA 3.11. *$\Phi^{2,3}$ is full.*

PROOF. Consider a partial deformation of $\mathfrak{D}^{2,3}$ into $\mathfrak{D}^{2,2}$ and $\mathfrak{D}^{2,1}$ by pulling out a vertical line (see Figure 5). In $\mathfrak{D}^{2,2}$, for every $n \in \mathbb{N}$, there is a ray in direction $(n, n+1)$

https://doi.org/10.1017/S000497272400128X Published online by Cambridge University Press

with function $(1 + t^{2n+1}x^n y^{n+1})^2$ (see Example 2.11). This intersects the pulled out vertical line, which has function $1 + ty$. By the change of lattice trick (Proposition 2.16), the diagram at the intersection corresponds to a standard diagram $\mathfrak{D}^{2n,n}$. By a full deformation, one easily sees that $\mathfrak{D}^{2n,n}$ has rays in directions $(1, 1), (1, 2), \ldots, (1, n)$, which correspond to rays in $\mathfrak{D}^{2,3}$ with directions $(n, n + 2), (n, n + 3), \ldots, (n, 2n + 1)$. Hence, for each direction (a, b) with $a \leq b \leq 2a + 1$, there exists a nontrivial ray in $\mathfrak{D}^{3,2}$. These include all directions with $1 \leq b/a \leq 2$. But this contains the fundamental region $\phi_0^{3,2}$, which lies between $\rho_{0,-}^{3,2} = 1$ and $\rho_{0,+}^{3,2} = \frac{3}{2}$. Therefore, $\phi_0^{3,2}$ is full, and so, by Lemma 3.8, $\Phi^{3,2}$ is full. □

LEMMA 3.12. *$\Phi^{1,5}$ is full.*

PROOF. Consider a partial deformation of $\mathfrak{D}^{1,5}$ to $\mathfrak{D}^{1,3}$ and $\mathfrak{D}^{1,2}$ (see Figure 5). As $c_{1,1}^{1,3} = 3$ (see Example 2.14), we get a subdiagram corresponding to $\mathfrak{D}^{3,2}$, with rays (a, b) in $\mathfrak{D}^{3,2}$ corresponding to rays $(a, a + b)$ in $\mathfrak{D}^{1,5}$. This maps the slope $\rho \mapsto \rho + 1$, so sends the dense region $\Phi^{3,2}$ between

$$\rho_{\pm}^{3,2} = \frac{6 \pm \sqrt{12}}{6} = 1 \pm \frac{1}{\sqrt{3}}$$

to the region between $2 \pm 1/\sqrt{3}$ in $\mathfrak{D}^{1,5}$. This contains the fundamental region $\phi_0^{1,5}$ which lies between $\rho_{0,-}^{1,5} = 2$ and $\rho_{0,+}^{1,5} = \frac{5}{2}$. So $\phi_0^{1,5}$ is full, and hence $\Phi^{1,5}$ is full by Lemma 3.8. □

Now Theorem 3.3 follows from Lemmas 3.11, 3.12 and Proposition 3.10.

3.4. Outside the dense region

PROPOSITION 3.13. *In a standard scattering diagram $\mathfrak{D}^{\mu,\nu}$, every ray with direction $(a, b) \in \mathbb{Z}_{>0}^2$ satisfies*

$$\frac{1}{\mu} \leq \frac{b}{a} \leq \nu.$$

PROOF. We show that $b/a \leq \nu$. Then $1/\mu \leq b/a$ follows by symmetry under exchanging (μ, a) and (ν, b). For $\nu = 1$, a full deformation of $\mathfrak{D}^{\mu,1}$ shows that only rays with slope $b/a \leq 1$ appear. Hence, we can assume that $\nu > 1$. We proceed by induction on $a + b$. The statement is clear for $a + b = 1$. For $a + b = 2$, we have $a = b = 1$, so $b/a = 1$, and the statement is also true. For $a + b > 2$, consider the partial deformation of $\mathfrak{D}^{\mu,\nu}$ into $\mathfrak{D}^{\mu,\nu-1}$ and $\mathfrak{D}^{\mu,1}$ by pulling out a vertical line. Consider the ray in $\mathfrak{D}^{\mu,\nu-1}$ with direction $(a_0, b_0) \in \mathbb{Z}_{>0}^2$. Its attached function is $(1 + t^{a_0+b_0}x^{a_0}y^{b_0})^{c_{a_0,b_0}^{\mu,\nu-1}}$. It intersects the pulled-out vertical line, which has function $1 + ty$. By the change of lattice trick (Example 2.17), the diagram at the intersection point is equivalent to $\mathfrak{D}^{a_0 c_{a_0,b_0}^{\mu,\nu-1}, a_0}$. It produces rays with directions $(a, b) = \alpha(a_0, b_0) + \beta(0, 1)$ for some $\alpha, \beta \in \mathbb{Z}_{>0}$. We have

https://doi.org/10.1017/S000497272400128X Published online by Cambridge University Press

$\alpha \le a$ and $\beta < b$, so $\alpha+\beta < a+b$ and $a_0+b_0 < a+b$. By the induction hypothesis, we have $\beta/\alpha \le a_0$ and $b_0/a_0 \le \nu - 1$. Then

$$\frac{b}{a} = \frac{\alpha b_0 + \beta}{\alpha a_0} = \frac{b_0}{a_0} + \frac{\beta}{\alpha}\frac{1}{a_0} \le \nu.$$

This completes the proof. □

PROPOSITION 3.14 (Theorem 1.4(b)). *Outside $\Phi^{\mu,\nu}$, the only rays that occur are those given by mutations of the initial rays. In particular, rays cannot be dense.*

PROOF. Let $\alpha_0 = 0, \alpha_1 = 1/\mu, \alpha_{n+1} = \mathbf{T}_2(\beta_n)$ and $\beta_0 = \infty, \beta_1 = \nu, \beta_{n+1} = \mathbf{T}_1(\alpha_n)$.

We know that there are no rays with slope $\alpha_0 < \rho < \alpha_1$ or $\beta_0 > \rho > \beta_1$, and, under mutations, if there are no rays with slope $\alpha_{n-1} < \rho < \alpha_n$ or $\beta_{n-1} > \rho > \beta_n$, then there are none with slope $\alpha_n < \rho < \alpha_{n+1}$ or $\beta_n > \rho > \beta_{n+1}$.

Note also that $\alpha_0 < \rho_-^{\mu,\nu}$ and $\beta_0 > \rho_+^{\mu,\nu}$ and that $\mathbf{T}_1, \mathbf{T}_2 : \rho_\pm^{\mu,\nu} \mapsto \rho_\mp^{\mu,\nu}$ are order reversing, so $\alpha_n < \rho_-^{\mu,\nu}$ and $\beta_n > \rho_+^{\mu,\nu}$. So we get bounded monotone sequences α_n, β_n and they converge to α, β, respectively. As $\mathbf{T}_2\mathbf{T}_1$ is continuous and maps α_n to α_{n+2} and β_n to β_{n+2}, respectively, α, β must be fixed points of $\mathbf{T}_2\mathbf{T}_1$. But the fixed points of

$$\mathbf{T}_2\mathbf{T}_1 : \rho \mapsto \nu - \frac{1}{\mu - 1/\rho}$$

are exactly $\rho_\pm^{\mu,\nu}$. So $\alpha = \rho_-^{\mu,\nu}$ and $\beta = \rho_+^{\mu,\nu}$, and we get the claim. □

Acknowledgements

This paper grew out of a Summer Research in Mathematics project carried out at the University of Cambridge. We are grateful to Dhruv Ranganathan for bringing us together and Markus Reineke for clarifying some questions about quiver representations. We thank the anonymous referee for carefully reading our paper and making important comments and suggestions.

References

[1] H. Argüz and M. Gross, 'The higher-dimensional tropical vertex', *Geom. Topol.* **26** (2022), 2135–2235.
[2] P. Bousseau, 'The quantum tropical vertex', *Geom. Topol.* **24**(3) (2020), 1297–1379.
[3] P. Bousseau, 'Scattering diagrams, stability conditions, and coherent sheaves on $\mathbb{P}^2$', *J. Algebraic Geom.* **31** (2022), 593–686.
[4] P. Bousseau, A. Brini and M. van Garrel, 'Stable maps to Looijenga pairs', *Geom. Topol.* **28** (2024), 393–496.
[5] T. Bridgeland, 'Scattering diagrams, Hall algebras and stability conditions', *Algebr. Geom.* **4**(5) (2017), 523–561.
[6] T. Gräfnitz, 'Tropical correspondence for smooth del Pezzo log Calabi–Yau pairs', *J. Algebraic Geom.* **31**(4) (2022), 687–749.
[7] M. Gross, P. Hacking and S. Keel, 'Mirror symmetry for log Calabi–Yau surfaces I', *Publ. Math. Inst. Hautes Études Sci.* **122** (2015), 65–168.
[8] M. Gross, P. Hacking, S. Keel and M. Kontsevich, 'Canonical bases for cluster algebras', *J. Amer. Math. Soc.* **31**(2) (2018), 497–608.

https://doi.org/10.1017/S000497272400128X Published online by Cambridge University Press

[9] M. Gross and R. Pandharipande, 'Quivers, curves, and the tropical vertex', *Port. Math.* **67**(2) (2010), 211–259.
[10] M. Gross, R. Pandharipande and B. Siebert, 'The tropical vertex', *Duke Math. J.* **153**(2) (2010), 297–362.
[11] M. Gross and B. Siebert, 'From real affine geometry to complex geometry', *Ann. of Math. (2)* **174**(3) (2011), 1301–1428.
[12] M. Gross and B. Siebert, 'The canonical wall structure and intrinsic mirror symmetry', *Invent. Math.* **229** (2022), 1101–1202.
[13] M. Kontsevich and Y. Soibelman, 'Affine structures and non-Archimedean analytic spaces', in: *The Unity of Mathematics*, Progress in Mathematics, 244 (eds. P. Etingof, V. Retakh and I. M. Singer) (Birkhäuser, Boston, MA, 2006), 321–385.
[14] M. Kontsevich and Y. Soibelman, 'Stability structures, motivic Donaldson–Thomas invariants and cluster transformations', Preprint, 2008, arXiv:0811.2435.
[15] M. Reineke, 'The Harder–Narasimhan system in quantum groups and cohomology of quiver moduli', *Invent. Math.* **152** (2003), 349–368.
[16] M. Reineke, 'Poisson automorphisms and quiver moduli', *J. Inst. Math. Jussieu* **9**(3) (2010), 653–667.
[17] M. Reineke, 'Cohomology of quiver moduli, functional equations, and integrality of Donaldson–Thomas type invariants', *Compos. Math.* **147**(3) (2011), 943–964.
[18] M. Reineke and T. Weist, 'Refined GW/Kronecker correspondence', *Math. Ann.* **355** (2013), 17–56.

TIM GRÄFNITZ, Institut für Algebraische Geometrie,
Leibniz-Universität Hannover, Welfengarten 1, 30167 Hannover, Germany
e-mail: graefnitz@math.uni-hannover.de

PATRICK LUO, Department of Pure Mathematics and Mathematical Statistics,
University of Cambridge, Wilberforce Road, Cambridge CB3 0WB, UK
e-mail: pl485@cam.ac.uk

https://doi.org/10.1017/S000497272400128X Published online by Cambridge University Press